Control of Flow Separation by Acoustic Excitation

M. Nishioka,* M. Asai,† and S. Yoshida‡
University of Osaka Prefecture, Sakai, Osaka 591 Japan

To control the leading-edge flow separation on an airfoil by means of acoustic excitation, the response to the incident sound and the resulting flow instability are studied experimentally and theoretically on the basis of the linear stability theory, for a flat-plate airfoil, at a chord Reynolds number $R_c = 4 \times 10^4$. Good agreement is shown on the instability characteristics; these experimental and theoretical results demonstrate that the separated shear flow is extremely unstable to small-amplitude disturbances and rolls up to form discrete vortices. The experiment also shows that the rolled-up vortices with appropriate scales and frequencies (less than that of the maximum linear amplification) work well to enhance the entrainment to reattach the separated shear layer. Through controlling the leading-edge separation, it is found that the maximum *u* fluctuation associated with the vortices can be 30–40% of the freestream velocity, and these strong vortices decrease the separation bubble in size down to one-third of the unexcited case, for the angle of attack up to 14 deg examined.

Introduction

IT is well known that the maximum lift available for a given airfoil is limited by the occurrence of the boundary-layer separation. When the angle of attack is increased beyond this limit, the separated shear layer forms a large-scale unsteady wake. This is the stall with a sudden decrease in lift and a steep rise in drag. It is highly desirable to have effective means of controlling the boundary layer to prevent the separation. The most well known among those in use for commercial airplanes is the vortex generator. The strong streamwise vortices behind the generator serve to increase the otherwise limited influx of momentum and energy toward the wall through enhancing the mixing between the energetic freestream and the boundary layer. The device works well, but not without a serious problem, that is, a high drag penalty.

Recently, the so-called acoustic excitation has received much attention as a new means for separation control. The advantage is its feasibility in wide application not restricted to the case of airfoil. Ahuja et al.[1] and Ahuja and Burrin[2] reported that the separation occurring on an airfoil can be suppressed by sound waves radiated at appropriate frequencies, as stated by Zaman et al.,[3] who observed the same effect. However, the suppression mechanism has not been established. This is undoubtedly the case because it is rather difficult to understand the receptivity process through which vortical disturbances are excited by sound waves. In Nishioka and Morkovin[4] it is proposed that a likely effective receptivity rests on the fact that the unsteady vorticity field (not unlike Stokes layer), due to sound waves, can introduce additional characteristic lengths other than their wavelengths, which can match the scale of the vortical disturbance to be excited under particular flow conditions. Subsequently, Goldstein[5] theoretically examined the relation between the intensities of the external sound-wave-like disturbance and the excited vorticity wave.

The instability of the separated shear layer is quintessential as the underlying mechanism that enables the sound waves to suppress the separation. Once the sound waves generate the unsteady vorticity field of the matched scale, the instability is triggered and the shear layer starts to roll up into discrete vortices. In other words, it is expected that the sound waves can control the scale and intensity of the vortices through the receptivity process. When the vortices and the associated flow structure thus excited really serve to enhance the entrainment and maintain the necessary influx of momentum toward the wall region, the separation is suppressed. With this in mind, the present authors decided to obtain some information on the following important points closely related to the receptivity and the suppression effect: 1) the maximum intensity of the vortices realizable by the acoustic excitation, 2) the spatial scale of the vortices most effective in suppressing the separation, and 3) the possible differences in the scale and intensity between the naturally growing vortices and the most effective vortices excited by sound waves.

In the present study, to examine these points, we have tried the acoustic excitation to suppress the flow separation at the leading edge, a literally sharp knife edge of a flat-plate airfoil. Generally speaking, when sound waves go around a corner and accelerate fluid elements (air), vorticity is induced there because of a no-slip condition. The greater the acceleration, the larger the sound-induced vorticity. The scale of the vorticity field is also determined by that of the related pressure gradient. Thus, expecting the most effective receptivity at the knife-edge, the sound waves are radiated almost perpendicularly to the airfoil surface. It is also noted that the sharp knife edge is the most receptive geometry to sound waves thus radiated.

Experimental Setup and Procedure

As illustrated in Fig. 1, the whole experiment is carried out using an open wind tunnel 200 mm × 200 mm in cross section. The freestream wind speed U_∞ can be varied continuously up to the maximum available, about 9 m/s. The freestream is fixed at 4 m/s for the present experiment. The flat-plate airfoil (aluminum) used is 150 mm in chord length, 197 mm in span, and 2 mm in maximum thickness. A sharp steel knife is glued on the plate to form the leading edge. The airfoil is supported at a distance of 100 mm from the leading edge, and the angle of attack α can be varied continuously. The chord Reynolds number R_c is about 4×10^4 at $U_\infty = 4$ m/s. Hot-wire measurements indicate that the nonuniformity in the freestream is within 2% at the tunnel exit and the residual turbulence is at most 0.3% in terms of *u* fluctuation at $U_\infty = 4$ m/s. The most turbulence energy is contained in the range of frequency below 50 Hz: the fan noise (of about 282 Hz) is less than 0.01%. A loudspeaker, working as the acoustic source, is provided below the airfoil, which is a 30-cm woofer, and the maximum input power is 125 W. Because the sound waves are radiated at almost a right angle to the airfoil as already noted,

Presented as Paper 89-0973 at the AIAA 2nd Shear Flow Conference, March 13–16, 1989; received July 18, 1989; revision received Dec. 7, 1989. Copyright © 1990 by the American Institute of Aeronautics and Astronautics, Inc. All rights reserved.

*Professor, Aeronautical Engineering. Member AIAA.
†Research Associate, Aeronautical Engineering.
‡Graduate Student, Aeronautical Engineering.

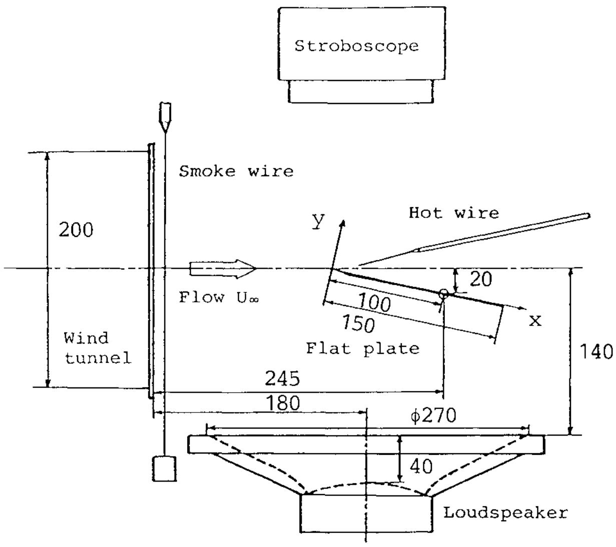

Fig. 1 Test section (dimensions in mm).

the possible minute vibration of the leading edge (none visible) but if any, gives no serious problems. The smoke wire of 0.1-mm-diam stainless steel and the stroboscope are for the flow visualization. It should be noted that a pair of large side walls of Plexiglas (400 mm × 700 mm) maintain the two dimensionality of the mainstream, though above and below the airfoil is opened to avoid the otherwise possible acoustic resonance.

In addition to hot-wire measurements for the time-mean velocity U and the fluctuation u in the x direction along the airfoil, the intermittency for the occurrence of reversed flow is measured using a pair of hot wires (placed at a distance of 0.7 mm apart), one of which operates as a sensor detecting the heat released from the other and carried by the reversed flow. We may call the intermittency γ, thus measured, the rate of reversed flow; the flow is reversed all the time when $\gamma = 1.0$, and there is no reversed flow when $\gamma = 0$.

After ascertaining that the time-mean flow is two dimensional for each run, detailed hot-wire measurement and visual observations are made in the spanwise center plane.

Natural Flow Without Acoustic Excitation

When the airfoil is set parallel to the mainstream at the angle of attack $\alpha = 0$ deg, the flow along the airfoil remains laminar down to the trailing edge without any appreciable separation. The local Reynolds number based on the displacement thickness is about 350 at the trailing edge, which is less than the critical for the growth of Tollmien-Schlichting waves. Under the natural flow conditions (without acoustic forcing by loudspeaker), flow visualization is done by means of smoke wire for the angle of attack up to 14 deg. The results are shown in Fig. 2. Already at $\alpha = 2$ deg, the flow separates at the leading edge. Wave disturbances appear in the separation bubble and roll up into discrete vortices downstream. As clearly observed at $\alpha = 4$ and 6 deg, reattachment to the wall is governed by the vortices. Through further growth and amalgamation, they lead to the development of a turbulent boundary layer, in particular at $\alpha \geqq 4$ deg. It should also be noted that discrete vortices develop in the bubble region beyond $\alpha = 6$ deg, and besides the phenomenon of amalgamation, there seems to be a certain mechanism producing periodic, large-scale vortical structures as evidenced on the photographs for $\alpha \geqq 6$ deg. Measurements of y distributions of the mean velocity U as well as those of the reversed flow rate γ indicate that the reattachment is possible only for $\alpha \leqslant 12$ deg under the natural flow conditions.

The mean flowfield in the separation bubble region is illustrated in Fig. 3 for the case of $\alpha = 8$ deg by plotting y distributions of U at x (distance along the airfoil from the leading edge) = 1–6 mm. The reversed flow is represented by solid circles. The natural growth of u fluctuation in the separated region is illustrated in Fig. 4, which shows u fluctuations at y positions of maximum shear at $x = 4$, 6, and 8 mm. The traces at three different z positions are compared in each photograph. From these traces we notice that the frequency of growing disturbances is in the range from $f = 500$ Hz to 600 Hz. In this connection it is interesting to see whether the initial growth of these natural disturbances is predicted by the linear stability theory. This will be discussed later. It should be noted that the maximum rms value in the y distribution of the total u fluctuation observed at $\alpha = 8$ deg is 8, 15, 23, 20, and 17% of U_∞ at $x = 6$, 10, 20, 30, and 50 mm, respectively. A similar feature is also observed at $\alpha = 14$ deg, where the separated layer does not reattach and the maximum rms value is 17, 24, and 25% of U_∞ at $x = 10$, 30, and 50 mm, respectively. In order to suppress the separa-

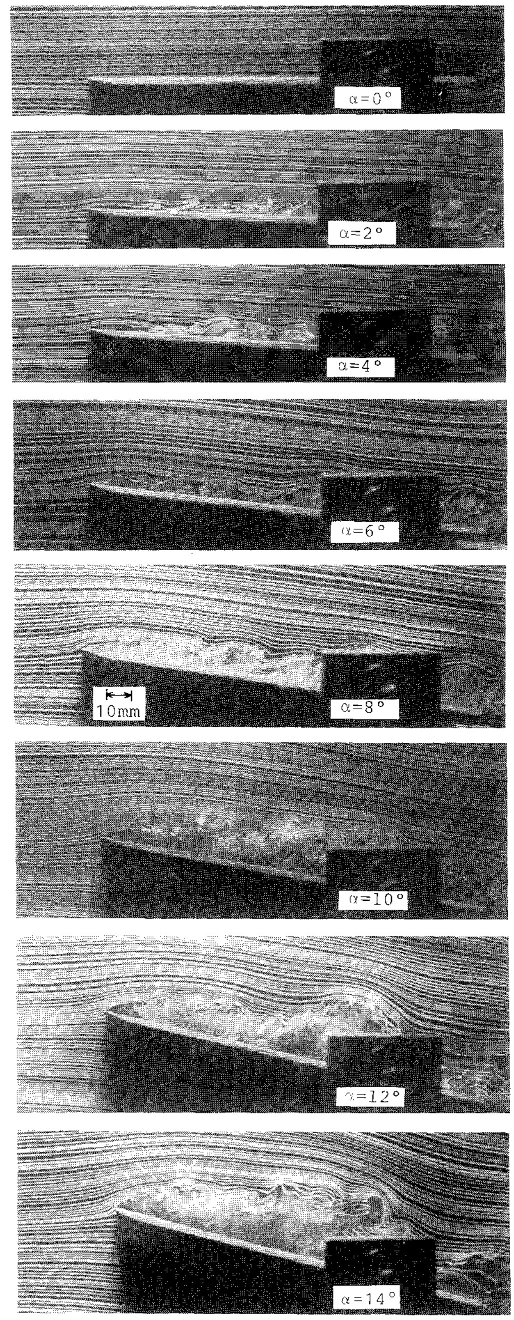

Fig. 2 Flow past a flat-plate airfoil at $U_\infty = 4$ m/s ($R_c = 4 \times 10^4$).

tion, more energetic vortical structures are needed to be excited as close to the leading edge as possible. This will be tried later.

Instability of Separated Shear Layer

To examine the instability of the leading-edge-separated shear layer minutely, the loudspeaker is driven to introduce controlled, initially weak disturbances, with the input power kept as low as an order of 0.03 W. The angle of attack α is set at 8 deg. The frequency f is varied from 200 Hz to 1000 Hz. For each run, y distributions of the bandpass filtered u fluctuation u_f are measured at various x stations. In Fig. 5 the maximum rms value u'_{fm} scaled with U_∞ is plotted against x for all of the frequencies examined; the ordinate is logarithmic. As the figure shows, the growth of these small-amplitude disturbances is almost exponential; and the growth rate is quite large, particularly at the frequencies between 400 Hz and 600 Hz, in agreement with the fact that the disturbances of these frequencies grow under the natural conditions, being triggered by freestream turbulence.

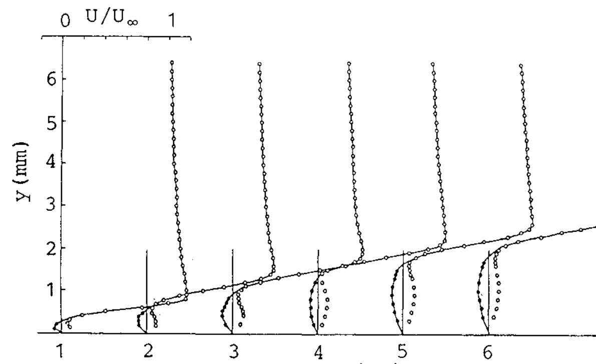

Fig. 3 Mean velocity distributions near the leading edge at $\alpha = 8$ deg: solid circles represent reversed flow.

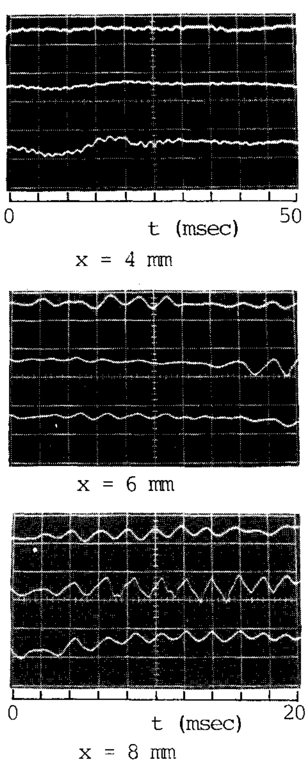

Fig. 4 Development of disturbances in the separation bubble region at $\alpha = 8$ deg; three traces in each photograph show the u fluctuations at three different z positions (equally spaced by 10 mm); vertical scale: $0.5U_\infty$/division.

To examine the instability theoretically, the stability calculation is made on the basis of the Rayleigh equation by assuming parallel flow. The velocity distribution at $x = 4$ mm (shown in Fig. 3) is selected as the basic flow for the stability calculation. The y distribution is accurately represented by the following expression:

$$U/U_\infty = 1 - G(y)/G(0)$$

$$G(y) = -0.260[1 + e^{2(y+0.2)}]^{-1} + 1.692[1 + 0.2e^{5.5(y-1.8)}]^{-5}$$
$$-0.405[1 + 0.2e^{8(y-1.8)}]^{-5} - 0.183[1 + e^{2(y-3.2)}]^{-0.125}$$

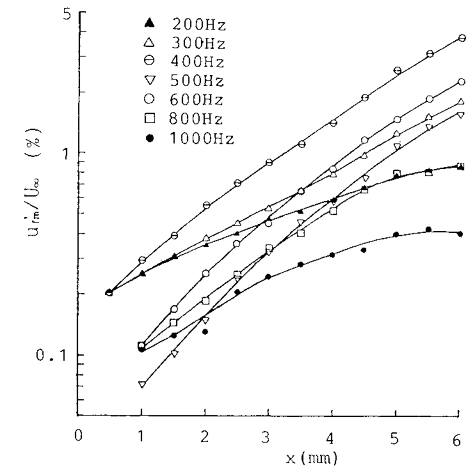

Fig. 5 Growth of small-amplitude disturbances excited by sound at $\alpha = 8$ deg.

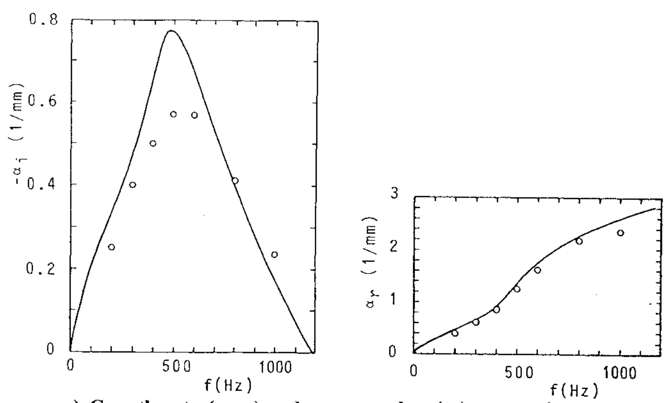

a) Growth rate ($-\alpha_i$) and wave number (α_r) at $x = 4$ mm

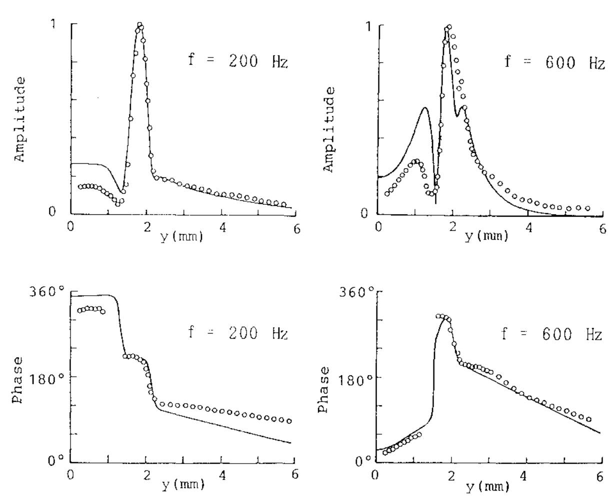

b) Amplitude and phase distributions of u fluctuation at $x = 4$ mm

Fig. 6 Comparisons of structure and behavior of small-amplitude disturbances at $\alpha = 8$ deg between experiment (○) and linear stability theory (——).

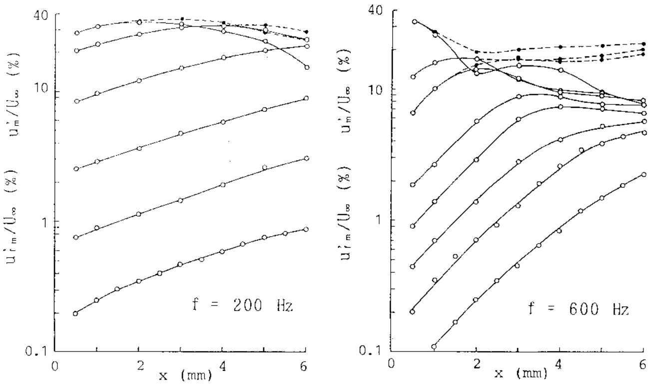

Fig. 7 Development of acoustically forced disturbances with various initial intensities at $\alpha = 8$ deg; ○; u_f, ●; total u.

The calculation made is of the spatially growing type, and the results are given in Figs. 6a and 6b, which, respectively, show the eigenvalues (growth rate $-\alpha_i$, wave number α_r) and the amplitude and phase distributions for $f = 200$ Hz and 600 Hz. These figures include the corresponding experimental results for comparison. The theoretical prediction agrees with the experimental results in all the aspects compared. This clearly indicates that the growth of disturbances is governed by the essentially inviscid inflectional instability, and the possible effect of highly nonparallel flow is almost negligible as far as the present comparisons are concerned.

Strong Disturbances Excited by Acoustic Forcing

As noted in the introduction, it is important to know the maximum intensity of the vortex realizable by the acoustic forcing. To answer this, the input power to the loudspeaker is changed systematically at $\alpha = 8$ deg, and the streamwise growth of the maximum intensity u'_m is examined at various frequencies. Typical results are given in Fig. 7: the maximum input power is 4.5 W and 2.0 W at $f = 200$ Hz and 600 Hz, respectively. The figures show that u'_m levels off near the leading edge when the forcing is the largest for each case. The near equilibrium surely indicates the formation of discrete vortices; this will be ascertained by flow visualization in Figs. 10. The maximum intensity attained at the formation is beyond $0.3U_\infty$ (in terms of u'_m) for $f = 200$ Hz, whereas it is below $0.2U_\infty$ for $f = 600$ Hz, in spite of the fact that the linear growth rate is much higher in the latter case as the same figures show. Figure 8 compares the developments of the corresponding u fluctuations at $f = 200$ Hz and 600 Hz. Soon after their formation, the discrete vortices seem to amalgamate themselves, as suggested by the intermittent occurrence of period doubling. This occurs earlier at $f = 600$ Hz than at $f = 200$ Hz. At the same time, breakdown occurs into three-dimensional, higher-frequency, smaller-scale eddies. These explain the earlier leveling off at $f = 600$ Hz followed by a rapid decrease in u'_{fm} (solid lines) beyond $x = 2$ mm, notwithstanding the continued slow growth in the total u'_m (dotted lines with solid circles). Suppose that a two-dimensional vortex forms on the wall along the leading edge, then, under the influence of the pressure gradient imposed by the vortex, the external flow will be forced around it to be entrained. The entrainment surely energizes the near-wall flow. This does not happen, however, unless the pressure gradient is large enough to counterbalance with the centrifugal force. Actually, when the vortex forms close to the wall, the resistive effects of the wall (on u and v) are significant and they set certain limits on the intensity of the vortex and the associated pressure gradient of the vortex. Thus, it is reasonable that the maximum intensity is lower for higher-frequency, smaller-scale vortices as shown by the comparison in Fig. 7 and by the plottings of the maximum intensity against frequency in Fig. 9 for $\alpha = 8$ and 12 deg. However, this feature is hard to imagine on the

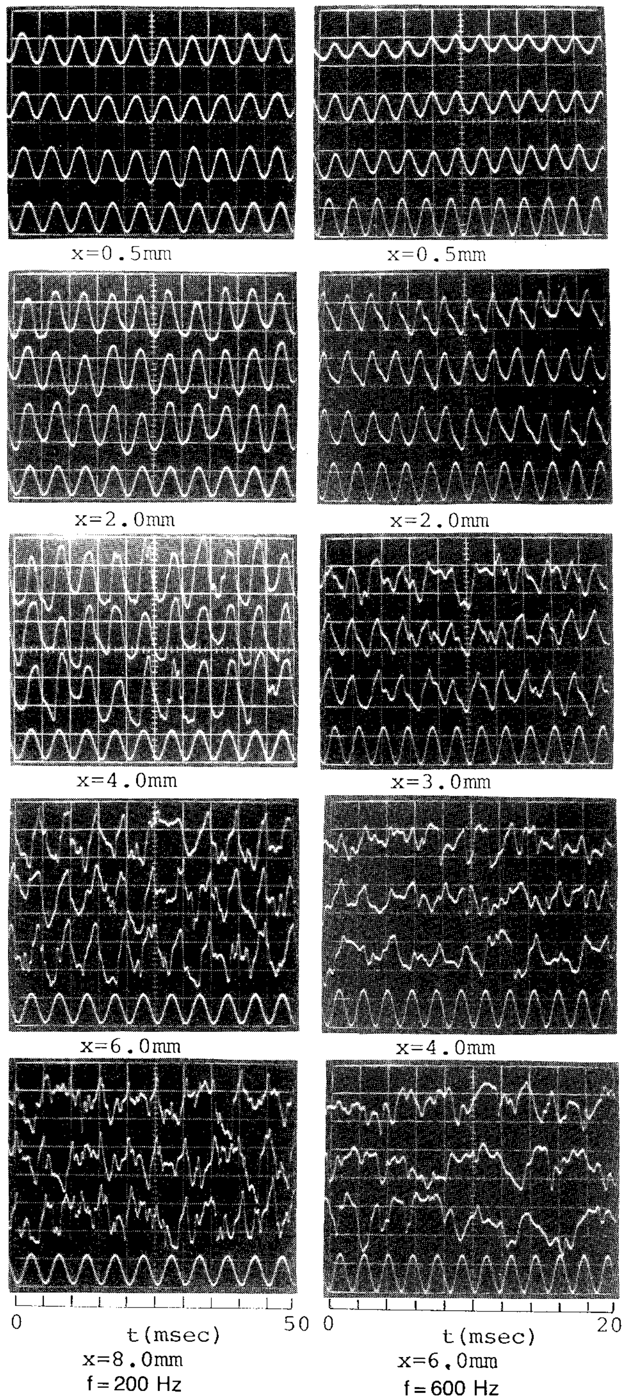

Fig. 8 Wave forms of u fluctuations acoustically forced at $\alpha = 8$ deg: u'_m/U_∞ at $x = 0.5$ mm is 20% and 14%, respectively, at $f = 200$ Hz and at $f = 600$ Hz; in each photograph, the upper three traces are u fluctuations at three z positions (equally spaced by 10 mm); the bottom is the driving signal; vertical scale: 0.5 U_∞/division.

basis of the growth rate vs frequency diagram given in Fig. 6a for small-amplitude disturbances. It never happens that the present weak freestream turbulence excites discrete vortices of frequencies below 400 Hz in the vicinity of the leading edge.

Acoustic Control of Leading-Edge Separation

To see the effects of sound-excited vortices in controlling the leading-edge separation, the flow visualization is made at $\alpha = 8$, 10, 12, and 14 deg at various forcing frequencies. The input power to the loudspeaker is adjusted to excite the vortices with the maximum intensity shown in Fig. 9. Figures 10 display the visualization photographs for $(\alpha, f) = (8$ deg, 200 Hz), (8 deg, 600 Hz), (12 deg, 200 Hz), and (12 deg,

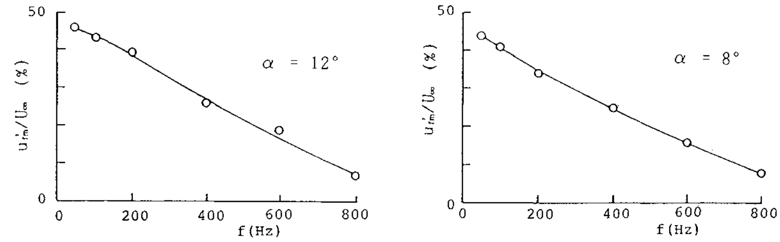

Fig. 9 Maximum rms intensity of vortices realizable by acoustic excitation; evaluated at $x = 2$ mm.

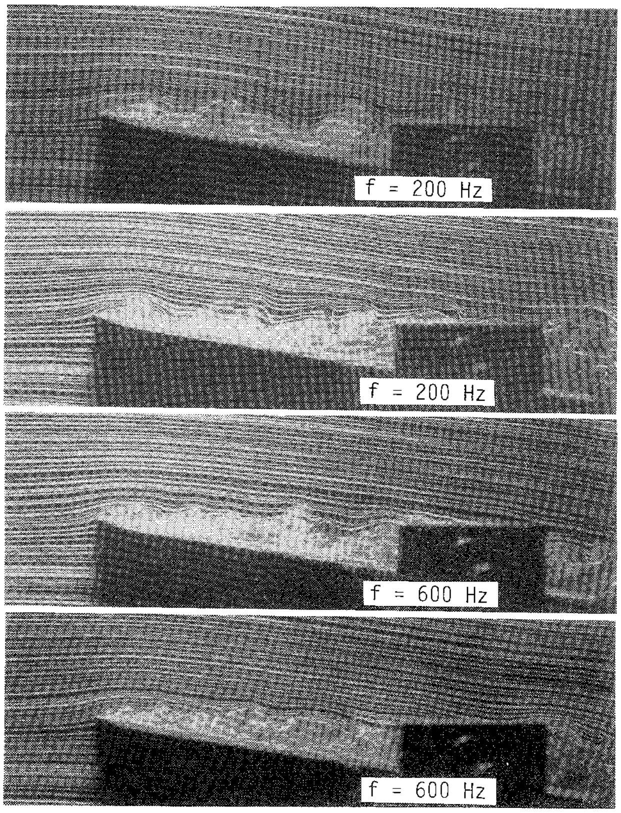

Fig. 10a Acoustic control of leading-edge separation at $\alpha = 8$ deg: compare these photographs with the corresponding unforced flows in Fig. 2.

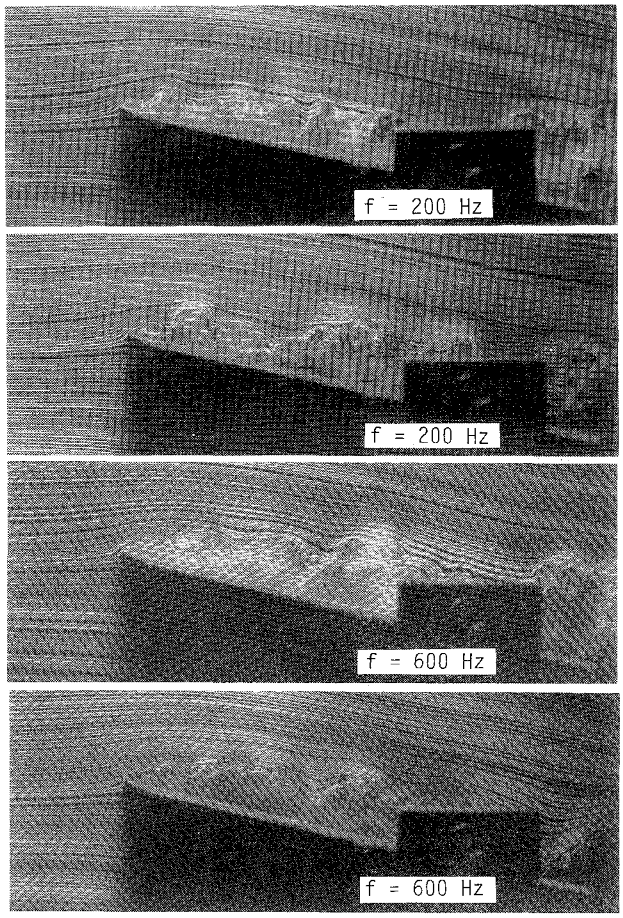

Fig. 10b Acoustic control of leading-edge separation at $\alpha = 12$ deg: compare these photographs with the corresponding unforced flows in Fig. 2.

600 Hz). These photographs clearly indicate that the separated shear layer rolls up into discrete vortices closer to the leading edge compared with the natural flow. These high-intensity vortices really serve to entrain the energetic external flow. Ready comparisons between the flows with and without excitations are possible in Fig. 11 at $\alpha = 14$ deg where the separated shear layer does not reattach without the forcing. In Figs. 10, we see that the forcing at 600 Hz is sufficiently effective when $\alpha = 8$ deg, more so than the forcing at 200 Hz. When $\alpha = 12$ deg, the situation is reversed, and we see more effective control at 200 Hz than at 600 Hz. The comparisons in Fig. 11 show that when $\alpha = 14$ deg, the forcing at 100 Hz is more effective than at 200 Hz. As for the scale of the effective vortex, these results indicate that it is scaled with the height of the shear layer from the wall (or the height of the separation bubble in the unforced flow). Indeed, the leading-edge vortex excited at 100 Hz is nicely matched to the region contoured by the shear layer (streak line extending from the leading edge) and the wall.

To show effects of acoustic forcing quantitatively, Fig. 12 illustrates the reversed flow region by means of γ = const lines for $\alpha = 12$ deg. The region enclosed by $\gamma = 0.5$ contour shrinks to about one-third when forced at 200 Hz. It is quite clear that the excitation is much more effective at 200 Hz than at 600 Hz. The mean flow measurements in Figs. 13 and 14 further ascertain that the leading-edge separation is surely suppressed by the present forcing, which excites energetic discrete vortices in the vicinity of the leading edge.

The fact that the acoustic forcing is effective in controlling the separation is no doubt due to the instability of the separated shear layer. Indeed, when the maximum rms intensity (of the discrete vortices) is about $0.35U_\infty$ at $f = 200$ Hz, the acoustic forcing (in terms of u) is only $0.03U_\infty$ at most, which is evaluated outside the vortical region near the leading edge up to $x = 2$ mm. However, the discrete vortices are formed right at the leading edge almost without a stage of growing travelling waves. At $f = 200$ Hz, the spacing between the successive vortices is almost two-thirds of the wavelength of the corresponding weak disturbance, indicating a nonnegligible difference from the linear instability.

The phenomenon of the almost direct rolling up from the leading edge is not unlike the so-called shedding from a

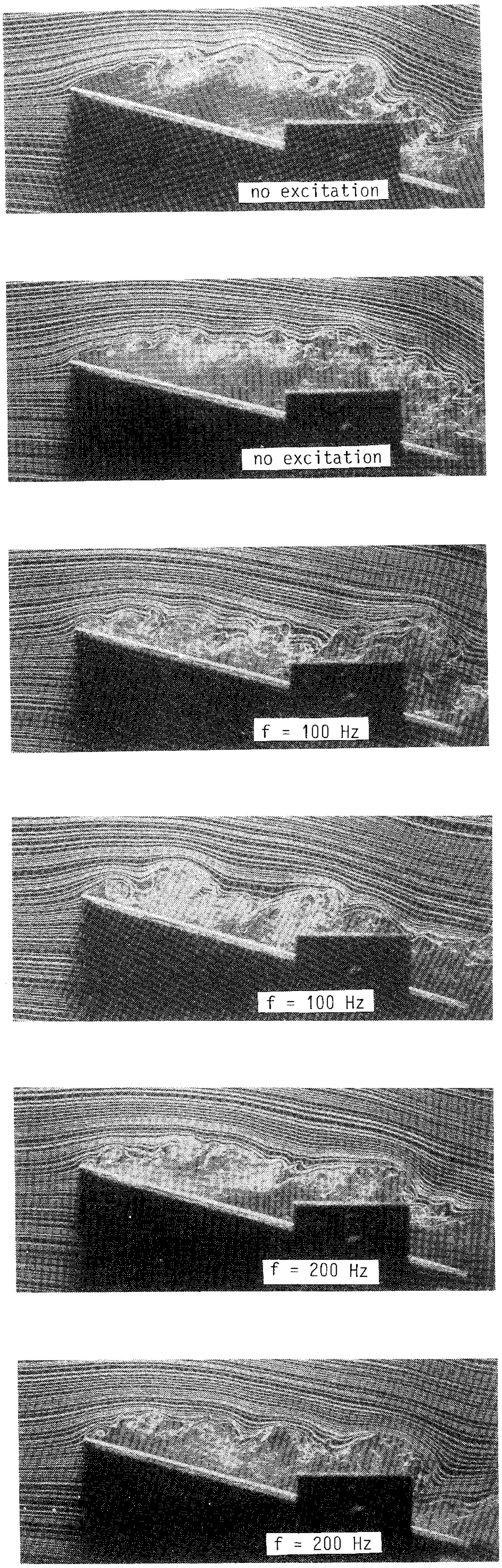

Fig. 11 Acoustic control of leading-edge separation at $\alpha = 14$ deg.

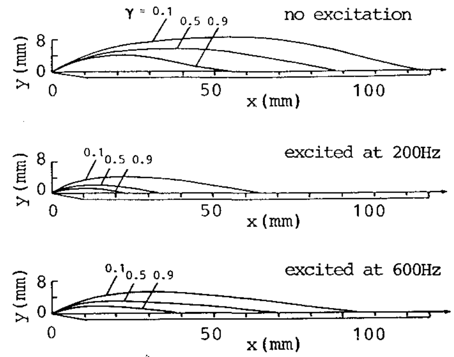

Fig. 12 Reversed flow region with and without excitation at $\alpha = 12$ deg, represented by contours of $\gamma = \text{const}$.

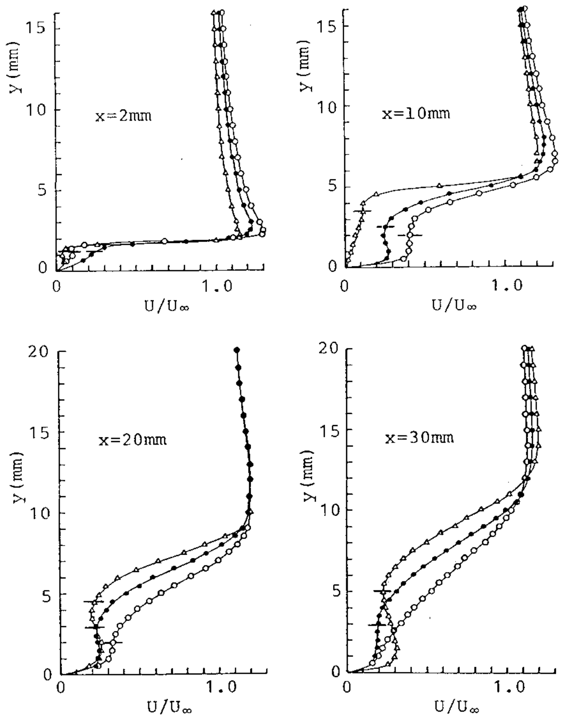

Fig. 13 Mean velocity distributions with and without excitation at $\alpha = 12$ deg: the bar represents the y position of $\gamma = 0.5$; near the wall, each distribution has reversed flow except that at $x = 30$ mm for $f = 200$ Hz, but no correction is made on the hot-wire reading; △; no excitation, ○; excited at 200 Hz, ●; excited at 600 Hz.

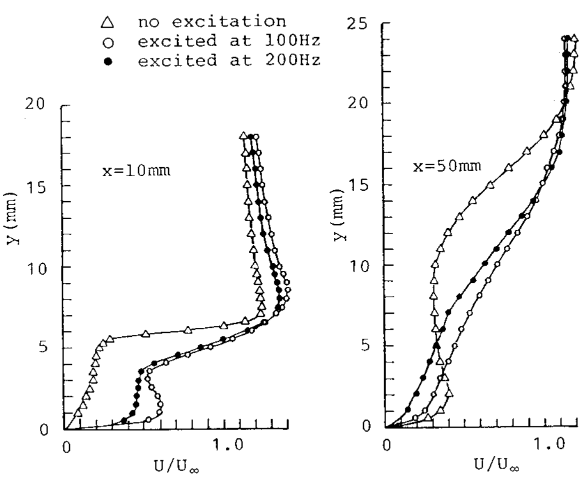

Fig. 14 Mean velocity distributions with and without excitation at $\alpha = 14$ deg: near the wall each distribution has reversed flow except that at $x = 50$ mm for $f = 100$ Hz and 200 Hz, but no correction is made on the hot-wire reading.

circular cylinder. In this connection, it is quite interesting that Sigurdson and Roshko[6] proposed the "shedding"-type instability and the related scaling law for the frequency. They studied the effect of a periodic velocity perturbation on the separation bubble downstream of the sharp-edged blunt face of a circular cylinder aligned coaxially with the freestream. The artificial velocity perturbation introduced at the sharp-edged corner could control the vortices developing in the bubble region. The flow could be considerably modified when the frequency of the forcing was lower than that of naturally growing waves due to the inflectional instability just as in the present experiment. The effective frequency is also found to be scaled with the height of the separation bubble as in the present experiment. They called the low-frequency instability the shedding type, considering the possible effect of the image vortex due to the nearby wall. We infer that some local feedback occurs through backflow and also through pressure waves from the vortical structures and their interaction (in particular their amalgamation) downstream. In this sense also, the direct rolling-up phenomenon is similar to the vortex shedding. So we would like to support the idea of Sigurdson and Roshko, though the details of the nonlinear instability needs to be clarified.

It must be further noted that Zaman et al.[3] cited in the introduction also observed the same effective forcing at a lower frequency discussed previously. Another important finding of Zaman et al.[3] is that high-frequency acoustic forcing (for instance, beyond 1000 Hz under present conditions) is effective in destroying large-scale vortices governing the stall phenomenon.

Conclusions

The leading-edge separation on a flat-plate airfoil is controlled by acoustic excitation at a chord Reynolds number 4×10^4. Because of its sharp leading edge, a clear separation bubble is already observed at the angle of attack $\alpha = 2$ deg. Special attention is focused on the receptivity and instability of the shear layer in the bubble region. The shear layer is found to be extremely unstable and to amplify small-amplitude disturbances into discrete vortices. The growing small-amplitude disturbances are well predicted by the linear stability theory when the calculation is made on the basis of the measured velocity distribution in the bubble, notwithstanding the fact that the flow is highly nonparallel. The naturally growing discrete vortices are efficient in enhancing the entrainment leading to the reattachment as long as their scale is matched to that of the bubble. As the bubble increases in size with an increasing angle of attack beyond $\alpha = 8$ deg, the naturally growing vortices become inefficient because of the mismatch in the scale mentioned: the naturally growing vortices are scaled with the thickness of the thin shear layer and almost independent of its height from the wall. The acoustic forcing is useful in exciting the discrete vortices of the matched scale right at the leading edge. The maximum rms intensity of the effective vortices realizable by acoustic excitation is found to depend critically on the frequency. It is more than $0.4U_\infty$ at the low-frequency limit (50 Hz) and around $0.1U_\infty$ at the high-frequency limit (800 Hz) examined.

References

[1]Ahuja, K. K., Whipkey, R. R., and Jones, G. S., "Control of Turbulent Boundary Layer Flows by Sound," AIAA Paper 83-0726, April 1983.

[2]Ahuja, K. K., and Burrin, R. H., "Control of Flow Separation by Sound," AIAA Paper 84-2298, Oct. 1984.

[3]Zaman, K. B. M. Q., Bar-Sever, A., and Mangalam, S. M., "Effect of Acoustic Excitation on the Flow over a Low-Re Airfoil," *Journal of Fluid Mechanics*, Vol. 182. Sept. 1987, pp. 127–148.

[4]Nishioka, M., and Morkovin, M. V., "Boundary Layer Receptivity to Unsteady Pressure Gradients: Experiments and Overview," *Journal of Fluid Mechanics*, Vol. 171, Oct. 1986, pp. 219–261.

[5]Goldstein, M. E., "Scattering of Acoustic Waves into Tollmien-Schlichting Waves by Small Streamwise Variations in Surface Geometry," *Journal of Fluid Mechanics*, Vol. 154, May 1985, pp. 509–529.

[6]Sigurdson, L. W., and Roshko, A., "The Structure and Control of a Turbulent Reattaching Flow," *Turbulence Management and Relaminarization,* edited by H. W. Liepmann and R. Narasimha, Springer-Verlag, Berlin, 1988, pp. 497–514.